Poultry Science

Electroporation-based Easi-CRISPR yields biallelic insertions of *EGFP-HiBiT* cassette in immortalized chicken oviduct epithelial cells

Lingkang Liu,[*,†,‡] Jinyu Wei,[*,§] Chen Chen,[*] Qianxue Liang,[*] Boyong Wang,[*] Wende Wu,[*,†,‡] Gonghe Li,[*,†,‡] and Xibang Zheng [*,†,‡,1]

[*]*College of Animal Science and Technology, Guangxi University, Nanning 530004, China;* [†]*Guangxi Zhuang Autonomous Region Engineering Research Center of Veterinary Biologics, Nanning 530004, China;* [‡]*Guangxi Key Laboratory of Animal Reproduction, Breeding and Disease Control, Nanning 530004, China; and* [§]*Buffalo Research Institute, Chinese Academy of Agricultural Sciences and Guangxi Zhuang Nationality Autonomous Region, Nanning 530004, China*

ABSTRACT Laying hens are an excellent experimental oviduct model for studying reproduction biology. Because chicken oviduct epithelial cells (**cOECs**) have a crucial role in synthesizing and secreting ovalbumin, laying hens have been regarded an ideal bioreactor for producing pharmaceuticals in egg white through transgene or gene editing of the ovalbumin (***OVA***) gene. However, related studies in cOECs are largely limited because of the lack of immortalized model cells. In addition, the editing efficiency of conventional CRISPR-HDR knock-in in chicken cells is suboptimal (ranging from 1 to 10%) and remains elevated. Here, primary cOECs were isolated from young laying hens, then infected with a retrovirus vector of human telomerase reverse transcriptase (**hTERT**), and immortalized cOECs were established. Subsequently, an electroporation-based **Easi-CRISPR** (Efficient additions with ssDNA inserts-CRISPR) method was adopted to integrate an *EGFP-HiBiT* cassette into the chicken *OVA* locus (immediately upstream of the stop codon). The immortalized cOECs reflected the self-renewal capability and phenotype of oviduct epithelial cells. This is because these cells not only maintained stable proliferation and normal karyotype and had no potential for malignant transformation, but also expressed oviduct markers and an epithelial marker and had a morphology similar to that of primary cOECs. EGFP expression was detected in the edited cells through microscopy, flow cytometry, and HiBiT/Western blotting. The *EGFP-HiBiT* knock-in efficiency reached 27.9% after a single round of electroporation, which was determined through genotyping and DNA sequencing. Two single cell clones contained biallelic insertions of *EGFP-HiBiT* donor cassettes. In conclusion, our established immortalized cOECs could act as an in vitro cell model for gene editing in chicken, and this electroporation-based Easi-CRISPR strategy will contribute to the generation of avian bioreactors and other gene-edited (**GE**) birds.

Key words: chicken oviduct epithelial cells, immortalization, electroporation, ovalbumin, Easi-CRISPR

2023 Poultry Science 102:103112
https://doi.org/10.1016/j.psj.2023.103112

INTRODUCTION

Producing therapeutic recombinant proteins by using animal bioreactors is a promising biotechnology for meeting the increasing demand for therapeutic proteins (Bertolini et al., 2016). Animal bioreactors are advantageous over cell culture systems because of their potential advantages of low cost and high production of pharmaceutical proteins (Hay et al., 2022). Antithrombin is the first pharmaceutical approved by the U.S. Food and Drug Administration (**FDA**). It was produced in the milk of transgenic goats (Kling, 2009). Later, mammal breast gland bioreactors were generated from rabbit (Kerekes et al., 2017), mice (Zeng et al., 2017), goat (Carneiro et al., 2018), and pig (Lee et al., 2020). However, various difficulties such as long timelines for reproduction and generation interval, complex biochemical composition of milk proteins, and difficult purification of recombinant proteins are associated with these bioreactors. Therefore, alternative animal bioreactors are expected to overcome these problems. The chicken oviduct bioreactor has several advantages over a mammalian expression system, including short incubation time (3 wk), short generation time (25 wk), lower feeding costs, facile flock expansion, higher protein yield, lower immunogenicity, and a glycosylation pattern similar to that of humans (Lillico et al., 2005; Bahrami et al.,

Received May 25, 2023.
Accepted September 8, 2023.

[1]Corresponding author: xibangzheng@gxu.edu.cn

2020). On December 8, 2015, a human lysosomal acid lipase, or Kanuma, the first pharmaceutical protein produced in the egg white of a transgenic hen, received FDA approval (Sheridan, 2016). Therefore, the chicken oviduct bioreactor can potentially be used in biomedicine.

Chicken ovalbumin (***OVA***) accounts for 54% of the total egg white in chicken eggs, and the *OVA* promoter strictly regulates its expression (Petitte and Mozdziak, 2007). By injecting lentiviral particles into chicken embryos at stage X, several transgenic chicken lines have been established. These transgenic hens can produce pharmaceutical proteins in egg white, such as ScFv-Fc mini-antibody and human interferon β1a (Lillico et al., 2007), human neutrophil defensin 4 (Liu et al., 2015), human lysozyme (Cao et al., 2015), human erythropoietin (Kwon et al., 2018), and human cytokine interferon α2a (Herron et al., 2018). However, lentiviral infection randomly integrates exogenous genes into the host genome and leads to a lower germline transmission of transgenes (Farzaneh et al., 2017). Moreover, this random integration may cause gene disruption in the host. Therefore, a more secure and efficient method must be identified for generating transgenic chicken with oviduct-specific expression of foreign genes.

Currently, zinc finger nucleases (**ZFNs**), transcription activator-like effector nucleases (**TALENs**), and clustered regularly interspersed short palindromic repeats (**CRISPR**) are widely used gene editing tools. CRISPR-associated protein 9 (**CRISPR/Cas9**) is an easier and more efficient genome editing tool than ZFNs and TALENs (Sampson and Weiss, 2014; Khalil, 2020). In the CRISPR/Cas9 system, the sgRNA−Cas9 complex creates double-stranded breaks (**DSBs**) in targeting sites, and nonhomologous end-joining (**NHEJ**) or homology-directed repair (**HDR**) pathway is involved in DSBs repair (Barman et al., 2020). The NHEJ pathway is prone to form indels (random insertions or deletions) and results in gene knock-out (**KO**), whereas the HDR pathway gives rise to the precise knock-in (**KI**) with homologous arms (**HAs**) (Ezaki et al., 2022). In a work by Dimitrov, using CRISPR-HDR, an additional loxP site was inserted into the chicken immunoglobulin heavy chain locus of the in vitro cultured primordial germ cells (**PGCs**) (Dimitrov et al., 2016). This is the first report of applying CRISPR-HDR in chicken cells. Thereafter, 2 GE hen lines were generated to produce human interferon beta (**hIFN-β**) and the heavy and light chains of humanized anti-HER2 (monoclonal antibody, **mAb**) in egg white (Oishi et al., 2018; Mukae et al., 2020). The KI hens were obtained by targeting *OVA*, and the procedure involved isolation and culture of PGCs, gene editing in vitro, and transfer of the edited cells back to embryonic blood. Nonetheless, the efficiency of CRISPR-HDR is lower (between 1 and 10%), and establishing PGC lines is technically sophisticated, time-consuming, and labor-intensive (Hagihara et al., 2020). Thus, improving the CRISPR-HDR KI efficiency in chicken and establishing an alternative cell model for chicken *OVA* editing in vitro are critical.

So far, many attempts have been made to improve the HDR efficiency. A study reported that the editing efficiency of HDR is enhanced when linear DNA is used as a repair template (Yamamoto and Gerbi, 2018). Additionally, single-stranded DNA (**ssDNA**) templates are more effective than double-stranded DNA (**dsDNA**) templates because of their lower cytotoxicity and higher integration efficiencies (Ranawakage et al., 2020; Gallagher and Haber, 2021). Furthermore, preparing ssDNA templates without DNA cloning is simple. Lately, a new gene editing strategy named Easi-CRISPR was used for editing mouse zygotes, where a mix of ssDNA donor and ribonucleoprotein (**RNP**) was injected into embryos, and the resulting KI efficiency was 30 to 60% (Quadros et al., 2017; Miura et al., 2018; Shola et al., 2021). Easi-CRISPR requires shorter HAs (55−105 bp) rather than longer HAs (500−1,000 bp) required in conventional CRISPR-HDR (Miura et al., 2018). To date, however, the application of Easi-CRISPR in chicken has not been reported.

Chicken oviduct epithelial cells (**cOECs**) are a useful cell model for determining the delivery efficiency of viral and nonviral constructs and for validating *OVA* promoter activity (Yang et al., 2021). Although cOECs are crucial for developing avian bioreactors to produce pharmaceutical proteins, no immortalized cOEC lines are available until now.

In this study, immortalized cOECs were obtained through hTERT retrovirus infection of primary cOECs, and Easi-CRISPR was used to insert an *EGFP-HiBiT* fusion cassette into the *OVA* locus of the immortalized cOECs through electroporation. The resulting KI efficiency was evaluated through monoclonal cell screening, genotyping, and HiBiT/Western blotting. This study thus facilitates the development of an avian bioreactor for producing recombinant pharmaceutical proteins in chicken egg whites.

MATERIALS AND METHODS

Experimental Animals and Animal Care

Laying hens were cared in accordance with animal welfare regulations and were purchased from the Guangxi Fufeng Agriculture and Animal Husbandry Co. Ltd. (Nanning, Guangxi, China). Athymic nude mice ($n = 6$, female, age: 5−8 wk) were purchased from Guangxi Medical University Laboratory Animal Center (Nanning, Guangxi, China). All animal experiments were approved by the Animal Care and Use Committee of Guangxi University, Guangxi, China (Authorization No. GXU 2019-041).

Isolation and Culture of cOECs

Approximately 25-wk-old laying hens were euthanized, and the oviduct tissue from the magnum was removed. The tissue was rinsed with phosphate-buffered saline (**PBS**) supplemented with 1% (v/v) penicillin and streptomycin (Solarbio, Beijing, China) and placed on a sterile petri dish. The mesosalpinx was trimmed,

and the oviduct tissue was dissected to expose the inner surface. The tissue was subsequently incubated with 1% (v/v) dithiothreitol (**DTT**, Merck, Darmstadt, Germany) to fully dissolve the mucus on the surface. After the tissue was washed with PBS, the part of mucosal folds was separated from the oviduct and minced into small tissue blocks by using ophthalmic scissors and forceps. The minced fragments were digested with 0.25% (v/v) Dispase II (Sigma-Aldrich) and placed in an incubator with 5% (v/v) CO_2 at 37°C for 60 min. The dispersed cells were filtered through a 40-μm nylon cell strainer (Fisher Scientific, Waltham, MA) and repeatedly pipetted using a 10-mL syringe with a 12G needle to further disperse the cells. This was followed by centrifugation at 1,500 rpm/min for 5 min. In the beginning of cell culture, fibroblast cell contamination was removed using a differential adhesion method (**DAM**) as previously reported (Kasperczyk et al., 2012). The roughly purified cOECs were grown in DMEM/F12 culture medium (Gibco, New York, NY) supplemented with 10% (v/v) fetal bovine serum (**FBS**, Gibco, New York, NY), 2% (v/v) chicken serum (Solarbio), 1% (v/v) penicillin-streptomycin (Solarbio), 5 ng/mL epidermal growth factor (GenScript, Nanjing, China), 5 μg/mL insulin (Solarbio) and 100 μmol diethylstilbestrol (Sigma-Aldrich). The cOECs were cultured at 37°C in a humidified incubator with 5% CO_2.

Generation of Immortalized cOEC Lines

Retroviral Production. The retroviral packaging cells Plat-GP were transfected with a recombinant retroviral vector pBABE-puro-hTERT (Addgene, #1771) and a packaging vector pCMV-VSV-G (Addgene, #8454). The Plat-GP cells at passage 2 were seeded onto a 10-cm culture dish coated with 0.01 g/mL polylysine and cultured in DMEM/F12 medium containing no FBS and penicillin-streptomycin. At approximately 75% confluence, the cells were transfected with 15 μg pBABE-puro-hTERT and 7.5 μg pCMV-VSV-G by using 67.5 μL polyethyleneimine transfection reagent (Sigma-Aldrich). The supernatants were collected after 48 h of transfection, filtered through a 0.45-μm strainer, and centrifuged at 32,000 rpm/min for 2 h. The retroviral pellet was resuspended in 0.9% saline solution and stored at −80°C until use.

Retroviral Tittering. Retrovirus titers were determined through serial dilution of virus-containing media on mouse embryonic fibroblasts NIH-3T3 (ATCC). NIH3T3 cells were grown in 24-well plates to 60% confluence and infected with 7 serial 10-fold dilutions of the recombinant retrovirus. After culture at 37°C for 24 h, another round of infection was conducted. At 48 h after infection, the medium was replaced with fresh culture medium for 2 to 3 d. The cell clones were observed and counted under a microscope. The virus titer was calculated as follows: Titer (CFU/mL) = (average number of cell clones)/(volume of diluted virus used per well) × (dilution factor).

Retroviral Transduction. According to the determined viral titer (4.8×10^6 CFU/mL), the optimal multiplicity of infection (**MOI**) for transducing cOECs was subsequently established. A series of MOI gradients (2.5, 5, 10, 20, and 40) were set, and the corresponding volume of retrovirus was calculated as follows: MOI = viral titer × virus volume/number of cells. Following retrovirus transduction and selection with puromycin, the resistant clones were observed under a microscope. The optimal MOI was determined as 10, this is because viability and morphology of the cell clones was at the best state when MOI = 10. To generate immortalized cell lines, cOECs at passage 2 to 3 were transduced with recombinant retrovirus (MOI = 10) in a 6-well plate and subjected to antibiotic selection with puromycin. First, cOECs were incubated for 5 h in DMEM/F12 culture medium containing the retrovirus and 4 μg/mL of polybrene (Solarbio). Then, the culture medium was replaced with fresh medium containing 1.0 μg/mL of puromycin (Sigma-Aldrich). After 8 d of screening, resistant colonies were transferred to individual wells of a 24-well culture plate and then to those of a 6-well culture plate, and finally to a 6-cm culture dish. The expanded cultures were frozen in liquid nitrogen for subsequent experiments.

Reverse Transcription-PCR Analysis

Total RNA from the primary and immortalized cOECs was prepared by using the TRIzol reagent (Takara, Kyoto, Japan) according to the manufacturer's instructions and then quantified using an ultraviolet spectrophotometer (Tiangen Biotech, Beijing, China). cDNA synthesis was performed with the PrimeScript II High Fidelity Reverse Transcription-PCR (**RT-PCR**) Kit (Takara). The mRNA expression of oviduct markers and hTERT were detected through RT-PCR. The markers included *OVA*, ovomucin (***OVM***), lysozyme (***LYZ***), and avidin (***AVD***). β-Actin (***ACTB***) was set as an internal control. The primers (Supplementary Table S1) were designed with NCBI Primer Blast and synthesized by Shanghai Bioengineering Corporation (Shanghai, China). The PCR conditions were as follows: predenaturation at 95°C for 5 min, 30 cycles of denaturation at 95°C for 30 s, annealing at 54°C for 30 s, elongation at 72°C for 30 s, and final elongation at 72°C for 5 min. The PCR products were resolved on 2% agarose gel through electrophoresis.

Immunofluorescence Staining

Immunofluorescence staining was performed to detect oviduct markers including the progesterone receptor (**PGR**), cytokeratin 18 (**CK18**), estrogen receptor 1 (**ESR1**), and OVA in both the primary and immortalized cOECs, as well as hTERT in the immortalized ones. The cells were seeded onto sterile coverslips in a 6-cm cell culture dish and cultured in the cOEC culture medium. At the 75% cell confluence, the coverslips were removed and transferred to an individual well of a 6-well

plate with the cell side faced up. After the cells were rinsed 3 times with PBS, they were fixed with 4% paraformaldehyde (Phygene, Fuzhou, China) and permeabilized with 0.5% Triton-X (Gibco) for 20 min at room temperature (**RT**, 25°C). The cells were blocked with 5% goat serum for 30 min at RT, incubated with a monoclonal or polyclonal anti-mouse/rabbit antibody (PGR/CK18/ESR1/OVA/hTERT, 1:250 dilution, Abcam, Cambridge, UK) overnight at 4°C in a humidified box, and incubated with fluorescein isothiocyanate (**FITC**)-conjugated rabbit anti-mouse/goat anti-rabbit IgG (1:2,000 dilution, Abcam, Cambridge, UK) for 60 min at RT. The cells were counterstained with DAPI (Beyotime, Shanghai, China). Finally, the coverslips were mounted using an antifade mounting medium (Solarbio) and observed under a fluorescent microscope (Nicon, Tokyo, Japan).

Colony Formation Test in Soft Agar

After preparing 1.2 and 0.7% agarose, the agarose was autoclaved and kept in a state of melting in water at 55°C. Then, 1.2% agarose was mixed with DMEM/F12 culture medium containing 20% FBS in a 1:1 ratio, added to a 6-well plate (1.5 mL/well), and allowed to solidify (as bottom glue) at RT. After trypsin digestion and centrifugation, the cell suspension of hTERT-cOECs at passage 50 or human cervical cancer cells (Hela, positive control) at a concentration of 5×10^4 cells/mL was prepared. The cocktail, composed of the cell suspension (100 μL/well) of hTERT-cOECs/Hela cells, and the mixture (100 μL/well) of 0.7% agarose and DMEM/F12 medium with 20% FBS were added to individual wells of the 6-well plate coated with the bottom glue. The cells were cultured at 37°C in a humified incubator with 5% CO_2, and the culture medium was supplemented every 3 d and stained with Giemsa to calculate the monoclonal formation rate after 3 wk of culture.

Teratoma Formation Test

The hTERT-cOECs or Hela cells (positive control) at the logarithmic growth stage was harvested through trypsinization and centrifugation at 1,000 rpm for 5 min. The cells were resuspended in serum-free DMEM/F12 medium at a concentration of 1×10^7 cells/mL. Six athymic nude mice were divided into 3 groups (2 mice in each group). Approximately 1×10^6 cells were injected subcutaneously into the axilla from the middle to posterior. The mice in the negative control group were injected with PBS alone. The mice were housed under specific pathogen-free conditions for 40 d. Tumor formation was observed, and tumor size was measured using vernier calipers.

Chromosome Karyotype Analysis

The cOECs were seeded into a 6-well culture plate and cultured in RPM1640 medium (Gibco) supplemented with 10% FBS and 1% penicillin-streptomycin. At 70 to 80% confluence of the cells, the medium was replaced with fresh RPM1640 medium supplemented with 0.2 μg/mL colchicine (Solarbio) for 2 h, and the cells were harvested through centrifugation at 1,000 rpm for 5 min. Subsequently, the cells were resuspended in 5 mL of hypotonic solution (0.075 M KCl), fixed in 10 mL of a fixative (acetic acid: methanol = 1:3 (v/v)), and dropped onto ethanol-cleaned slides. The slides were air dried and stored at −20°C. Finally, the slides were immersed for 10 min in a 10% Giemsa solution to stain chromosomes.

CRISPR sgRNAs Design and Synthesis

Using an online tool CHOPCHOP (http://chopchop.cbu.uib.no/), 200-bp DNA sequences of the chicken *OVA* around the stop codon (exon 8 of *OVA*) were analyzed, and 3 sgRNAs with high scores were selected to test the cutting efficiency.

The sgRNAs were prepared using a Guide-it sgRNA In Vitro Transcription Kit (#632635, Takara) according to the manufacturer's instruction and subsequently purified with the Guide-it IVT RNA Clean-Up Kit (#632638, Takara). sgRNA concentrations were determined using a spectrophotometer (Tiangen, Beijing, China), and their integrity was determined on 2% agarose gel through electrophoresis.

Cleavage Validation of CRISPR sgRNAs

A Guide-it Complete sgRNA Screening System (#6322639, Takara) was used to determine the cleavage efficiency. First, a DNA template covering 3 target sites was PCR amplified from chicken oviduct tissues by using a specific pair of primers (Supplementary Table S1). Second, a mixture of Cas9 proteins (50 ng/μL) and an *OVA* sgRNA (10 ng/μL) was incubated along with the DNA template (35 ng/μL) in a Cas9 nuclease reaction buffer at 37°C for 1 h. The reactions were stopped by incubating the mixture at 80°C for 5 min, and the digestion products were resolved on 2% agarose gel. Finally, the efficiencies of sgRNAs were determined through densitometry scanning using Image J (https://imageJ.net).

To further evaluate the efficacy of *OVA* sgRNAs, Cas9 proteins and in vitro transcribed *OVA* sgRNA were delivered into the hTERT-cOECs by using an electroporator (BTX ECM 830, Holliston, MA). The thawed cells were subjected to subculture at least for 3 passages before electroporation. For each electroporation, 0.2 μg of sgRNA and 1 μg of recombinant Cas9 (#632640, Takara) were mixed to prepare the RNP complex (molar ratio of approximately 1:1). The hTERT-cOECs were harvested with trypsinization and centrifugation, and resuspended in 100 μL Opti-DMEM medium (Gibco). The RNP complex was mixed with the cell suspension and added to an electroporation cuvette (2 mm gap). After electroporation, the cells were

transferred to new 12-well culture plates for another 72 h of culture. The genomic DNA was extracted from the electroporated cells by using a genomic DNA miniprep kit (Tianmobio, Beijing, China). DNA segments covering target sites were amplified using corresponding primer sets (Supplementary Table S1) and purified using an EZNA gel extraction kit (Omega, Norcross, GA). The PCR products were used for the T7 endonuclease I (**T7EI**) assay as previously reported (Miura et al. 2018). To further confirm indel formation, the PCR products were TA-cloned into a pMD18-T vector (#6011, Takara) for DNA sequencing.

Design and Generation of lssDNA for Novel DNA Insertion

To generate an HDR-based dsDNA donor, a small luminescent peptide tag called HiBiT was fused to the C terminal of an *EGFP* reporter. HiBiT is a part of NanoLuc luciferase and is unable to generate a strong luminescent signal until complemented with the remaining subunit (LgBiT). Therefore, the EGFP expression level could be quickly quantified by determining the NanoLuc luciferase activity. A self-cleaving peptide (*T2A*) was placed in the upstream of *EGFP* to allow endogenous *OVA* and *EGFP-HiBiT* to express independently at the protein level. The donor cassette (*T2A-EGFP-HiBiT*) was designed to be flanked with HAs of left and right (**HAL**/**R**) and inserted immediately upstream of the stop codon of *OVA*, keeping the donor in the same open reading frame with endogenous *OVA*. HAL, which consists of 623-nucleotides (**nt**), extends from the last amino acid of *OVA* to its upstream genomic sequence, while the 669-nt HAR spans the stop codon, 3′-UTR, and downstream genomic sequence. The assembled DNA donor consists of HAL + T2A + EGFP-HiBiT + Poly A + HAR, whose total length is up to 1.1 kb. The sense (top) strand of the dsDNA vector would be the optimal long ssDNA (**lssDNA**) donor for Easi-CRISPR.

To generate the dsDNA template, HAL and HAR were amplified from the genomic DNA of chicken OECs, and the stop codon-free *T2A-EGFP* was amplified from a cloning vector pMD 18T-*T2A-EGFP*. The sense and antisense DNA oligos of HiBiT were annealed and ligated to the site between *Bgl*II and *Hind*III of the pEGFP-C1 vector, from which the *HiBiT-polyA* fragment was amplified. Finally, T2A-EGFP and *HiBiT-polyA* were fused using the overlapping PCR technique. All PCR primers are listed in Supplementary Table S2. Subsequently, the dsDNA template (HAL-2A-EGFP-HiBiT-PolyA-HAR) was anchored in the plasmid pGolden-AAV (Addgene, #51424) by using the Golden Gate cloning method (Luo et al., 2014) (see Supplementary Figure S1). Finally, the lssDNA donor was prepared using the Guide-it Long ssDNA production system and Strandase kit (632644, Takara, Kyoto, Japan) according to the manufacturer's instructions. Briefly, a dsDNA donor cassette was PCR-amplified with an unmodified sense primer and a phosphorylated antisense primer. The resulting PCR products were digested by a strandase to degrade the undesired antisense strand and leave the sense strand for column purification. This purified lssDNA cassette was used for KI experiments.

Delivery of CRISPR Reagents and lssDNA Into the hTERT-cOECs

The Cas9 protein (25 pmol) was premixed with 25 pmol of in vitro transcribed *OVA* sgRNA and incubated at 37°C for 5 min to form the RNP complex. Then, the lssDNA (20 pmol) was added, and the RNP-lssDNA complex was formed after incubation for 2 h at 4°C. The hTERT-cOECs (1×10^6) were harvested and resuspended in BTXpress Cytoporation Media T4 electroporation buffer (BTX, Holliston, MA). The RNP-lssDNA complex was added to the hTERT-cOECs, and the resulting complex was transferred to an electroporation cuvette (2 mm gap). Electroporation was conducted under an empirically determined condition (160 V, single pulse, 5 ms). After electroporation, the cells were immediately moved to new 6-well culture plates and grown at 37°C in a humidified incubator with 5% CO_2. The cells were harvested after 48 to 72 h of culture.

Fluorescence Microscopy, Flow Cytometry, and Fluorescence-Activated Cell Sorting

All fluorescence images were acquired from the bright-field and green fluorescence channels by using a fluorescence microscope (Nicon Ti-S, Tokyo, Japan). The percentage of EGFP-positive cells was determined using the Accuri C6 Flow Cytometer (BD Biosciences, San Jose, CA) and Flow Jo software (version 10.6.2, Tree Star Inc., San Jose, CA). Cell sorting was performed using a fluorescence-activated cell sorting (**FACS**) Aria II flow cytometer (BD Biosciences, San Jose, CA).

Screening and Expanding Culture of EGFP+ cOECs

The sorted EGFP-positive (**EGFP**+) cOECs were used to screen monoclonal cells by using the limiting dilution method (**LDM**), followed by expanding culture. Briefly, the EGFP+ cOECs were diluted and seeded in 96-well plates at a density of 1, 5, 10, and 20 cell per well. After 24 h, the wells in which only a single cell appeared were marked. Then, these monoclonal cells were subcultured and expanded by transferring them to 24-, 12-, and 6-well culture plates step by step during 3 to 4 wk of culture. The expanded culture of EGFP+ cOECs were used for genotyping analysis.

Genotyping Analysis

Genomic DNA was extracted from the wild-type cOECs and monoclonal EGFP+ cOECs and used for genotyping analysis through PCR. Three pairs of

primers (Supplementary Table S1) were used to amplify 5′- and 3′-junction areas around the insertion site, as well as the full donor DNA cassette. The PCR products were resolved on 2% agarose gel. Furthermore, to further confirm the KI allele of *EGFP-HiBiT* in the *OVA* locus, the PCR products were TA-cloned to the pMD18-T vector for DNA sequencing.

HiBiT Blotting and Western Blotting

The proteins were extracted from the EGFP+ and wild-type cOECs by using RIPA lysis buffer (Beyotime) and quantified using a BCA protein assay kit (Beyotime). An equal amount of protein (50 mg each sample) was separated through sodium dodecyl sulfate-polyacrylamide gel electrophoresis and transferred onto a nitrocellulose membrane (Millipore, MA). For the HiBiT blotting assay, a Nano-Glo HiBiT blotting reagent containing the LgBiT protein and furimazine substrate was directly added onto the nitrocellulose membrane to visualize the luminescent signal by using a Syngene Chemi Genius Bio Imaging System (Syngene, Cambridge, UK). For the Western blotting assay, the nitrocellulose membrane was probed with polyclonal rabbit antichicken ovalbumin antibody (1:500 dilution, Sigma-Aldrich)/ anti-EGFP antibody (1:600 dilution, Absin, China)/ antihuman hTERT antibody (1:2,000 dilution, Absin, China). Finally, the nitrocellulose membrane was incubated with horseradish peroxidase (**HRP**)-conjugated goat anti-rabbit IgG (1:10,000 dilution, Abcam, Cambridge, UK). Using anti-β actin antibody (1:2,000 dilution, Abcam, Cambridge, UK) as an internal control, reprobing was performed. Immunoblotting bands were detected using a BeyoECL Plus reagent (Beyotime), captured using the Syngene Chemi Genius Bio Imaging System, and quantified through densitometry scanning.

Enzyme-Linked Immunosorbent Assay

The culture supernatant of KI cell clones and intact hTERT-cOECs was collected and quantified using a BCA protein assay kit (Beyotime). A commercial chicken OVA protein (Sigma-Aldrich) was used to draw a standard curve of the enzyme-linked immunosorbent assay (**ELISA**). A 10-fold serial dilution of the OVA standard was performed in TBST buffer, and the diluted OVA proteins were added to individual wells of 96-well plates (100 μL/well) to coat the wells. The remaining protein-binding sites were blocked by TBST solution containing 5% nonfat dry milk, and the OVA protein was probed with a polyclonal rabbit antichicken ovalbumin antibody (1:50,000 dilution, Sigma-Aldrich) in the coated wells. After incubation with an HRP-conjugated goat anti-rabbit IgG (1:10,000 dilution, Abcam, Cambridge, UK), a tetramethylbenzidine substrate (Sigma-Aldrich) was added to develop color, and the reaction was stopped with 2 N sulfuric acid. The absorbance from the duplicate of the standard was measured at 450 nm by using a microplate reader (Bio-Rad, Hercules, CA). A standard curve of ELISA was created by plotting the mean absorbance (Y axis) against the protein concentration (X axis) by using the Excel tool. Finally, the supernatant was diluted in TBST buffer at a final concentration of 20 μg/mL, and added to individual wells of 96-well plate (100 μL/well) to coat the wells. The ELISA assay was performed by following the aforementioned procedure. The OVA concentration in the supernatant was determined from the standard curve.

Cell Viability Assays

The Cell Counting Kit-8 (**CCK8**) assay (Beyotime) was used to evaluate the growth and proliferation of EGFP+ cOECs. Briefly, the cells were seeded in 96-well plates and cultured until they are tested at different time points (0, 12, 24, 48, 72, and 96 h). After 2 h of incubation with the CCK-8 reagent at 37°C with 5% CO_2, the absorbance was recorded at 450 nm by using the microplate reader.

Off-Target Analysis

The potential CRISPR/Cas9 off-target sites (**OTS**) were predicted simultaneously during sgRNA designing with CHOPCHOP. All OTS were located in introns or intergenic loci (Table 2). DNA segments around each candidate site for the T7EI assay were amplified through genomic PCR. The primer pairs are listed in Supplementary Table S1.

Statistical Analysis

Statistical analysis was performed using GraphPad Prism software (t test), and $P < 0.05$ indicates statistical significance.

RESULTS

Isolation, Culture, and Identification of cOECs

The cOECs were isolated from young hens through digestion with Dispase II and purified them through DAM. Biological characteristics of the cells were identified through morphological observation and surface marker detection. Morphologically, the primary cOECs are typically cobblestone-like at passage 0, whereas their number decreased by degrees. These cells gradually became fibroid with an increase in passage number (Figure 1A). The RT-PCR results showed that the primary cOECs were positive for some chicken oviduct-specific markers such as *OVA, OVM, LYZ*, and *AVD* (Figure 1B). Immunofluorescence staining revealed that primary cOECs were positive for the epithelial cell marker CK18 and for oviduct-specific markers such as OVA, PGR, and ESR1 (Figure 1C). In a word,

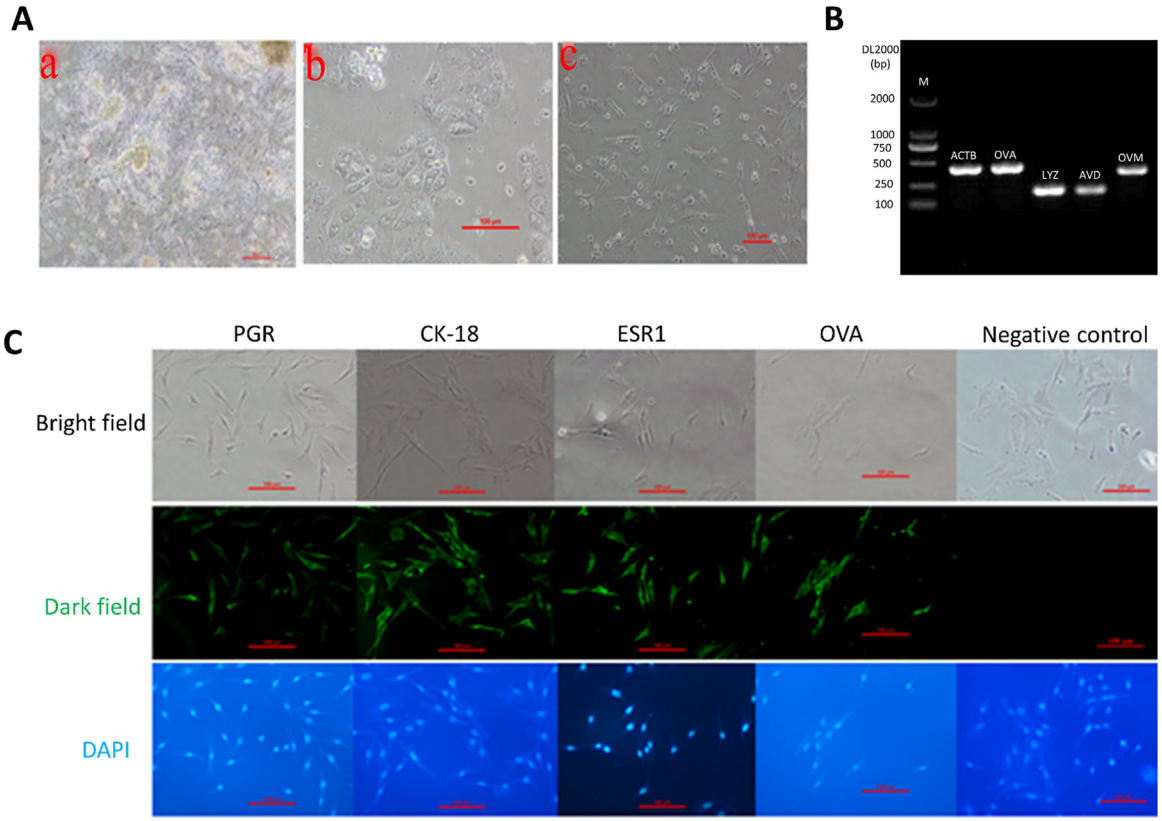

Figure 1. Characterization of the primary cOECs. (A) Images of the primary cOECs in culture at passage 0 (a), 1 (b), and 6 (c). Scale bar: 100 μM. (B) RT-PCR detection of oviduct markers. Total RNA was extracted from the primary cOECs, and the cDNA fragments of the markers (*OVA, LYZ, AVD*, and *OVM*) were amplified through RT-PCR and resolved in 2% agarose gel. ACTB served as a positive control. Lane M. DNA marker. (C) Immunofluorescence staining of the oviduct markers (OVA, ESR1, and PGR) and an epithelial cell marker (CK18) in primary cOECs. The primary cOECs were stained with a polyclonal or monoclonal antibody (OVA/ESR1/PGR/CK18), stained with a FITC-conjugated goat anti-rabbit/mouse IgG, and counterstained with DAPI. The primary cOECs were positive to all of the aforementioned markers. The group without antibody staining was set as a negative control. Scale bars: 100 μm.

morphological observation, and epithelial cell marker and oviduct marker detection indicated that the isolated cells were indeed cOECs.

Generation and Characterization of Immortalized cOECs

hTERT gene transfer has been used for immortalizing cells through telomere elongation. To obtain stable immortalized cOECs lines, the hTERT gene was introduced into the primary cOECs through retroviral infection. The immortalized cOECs, named hTERT-cOECs, were generated through puromycin screening and monoclonal cell culture after the retroviral infection. Primary cOECs and hTERT-cOECs were similar morphologically, and hTERT-cOECs could be stably subcultured for more than 50 passages with no senescence (Figure 2A). RT-PCR (Figure 2B), Western blotting assays (Figure 2C), and immunofluorescence staining (Figure 2D) revealed that hTERT was expressed in the hTERT-cOECs but not in the primary cOECs. Similar to the primary cOECs, the hTERT-cOECs were also positive for the epithelial cell marker (CK18) and oviduct markers (*OVA, PGR, ESR1, OVM, LYZ*, and *AVD*) (Figure 2E).

Chromosomal karyotyping demonstrated that both the primary cOECs and hTERT-cOECs maintained the normal diploid chicken chromosome ($2n = 78$) (Figure 3A). In the colony formation test, Hela cells readily formed colonies in soft agar, but the primary cOECs and the hTERT-cOECs did not. However, colonies of Hela cells were observed (Figure 3B). The teratoma formation test indicated that hTERT-cOECs did not give rise to teratoma formation, but Hela cells did (Figure 3C). Altogether, these results indicated that the hTERT-cOECs did not exhibit any potential for malignant transformation.

In Vitro Validation of Cleavage

The high cleavage efficiency of sgRNAs is a prerequisite for CRISPR-HDR KI. Three sgRNAs around the stop codon of the *OVA* gene were designed (Table 1 and Figure 4A), and the in vitro cutting efficiency of the sgRNAs was tested in hTERT-cOECs (Figure 4B–D). As shown in Figure 4B, the cutting efficiencies of the selected sgRNAs were 70.7% for sgRNA1, 94.6% for sgRNA2, and 87.1% for sgRNA3. To obtain consistent cleavage efficiencies, 3 tested sgRNAs with Cas9 protein were electroporated to the hTERT-cOECs for the T7EI assay, and the

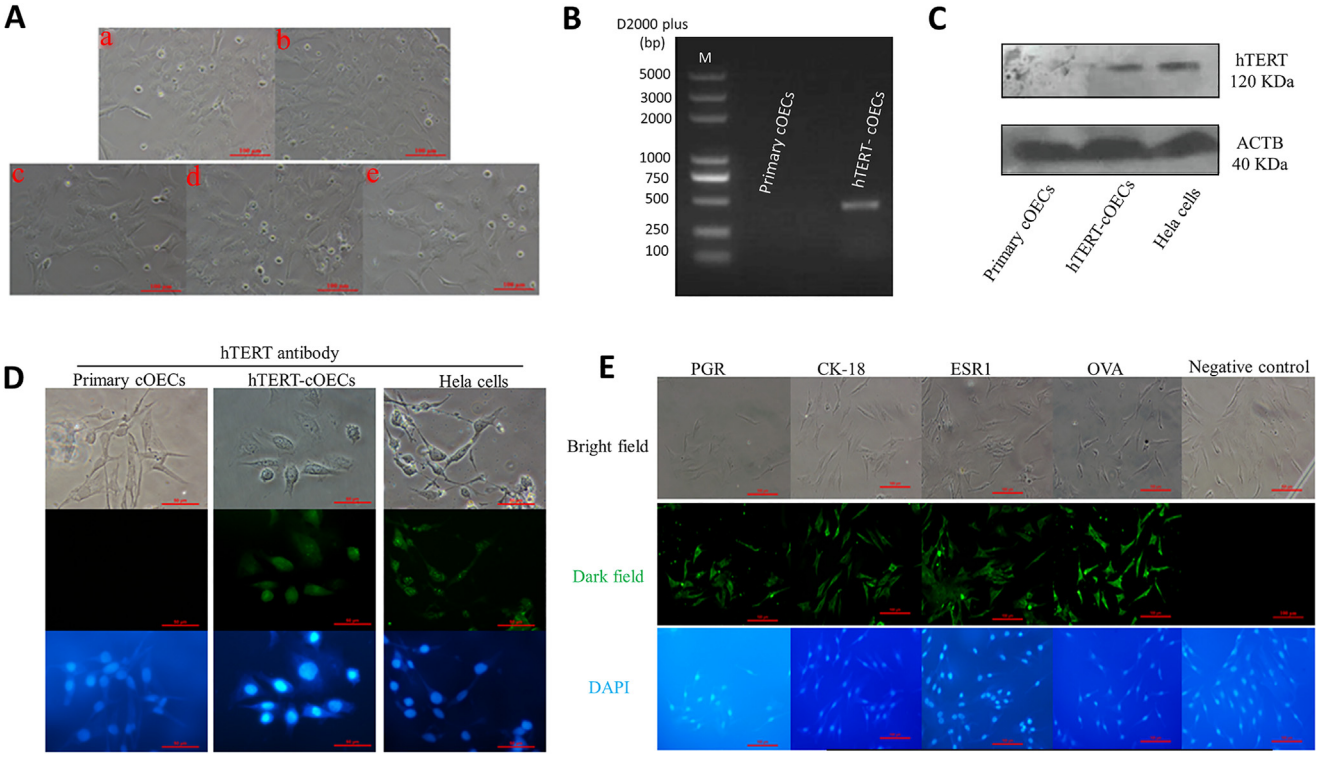

Figure 2. Characterizations of the immortalized hTERT-cOECs. (A) Images of the hTERT-cOECs at passage 10 (a), 20 (b), 30 (c), 40 (d), and 50 (e). Scale bar: 100 μM. The hTERT expression assay of hTERT-cOECs was conducted in B, C, D. (B) RT-PCR detection of hTERT mRNA expression in the hTERT-cOECs. A 0.4-kb hTERT fragment was detected in the hTERT-cOECs, but not in the primary cOECs. (C) Detection of hTERT expression through Western blotting. Protein samples were prepared from the immortalized/primary cOECs, and Hela cells were used for the Western blotting assay. A specific band was detected in Hela cells (positive control) and the hTERT-cOECs, but not in the primary cOECs (negative control). ACTB served as an internal control. (D) Immunofluorescence staining of hTERT antibody. The hTERT-cOECs and Hela cells were positive to hTERT, while the primary cOECs were not (negative control). Scale bars: 50 μm. (E). Immunofluorescence staining of oviduct markers in hTERT-cOECs. Similar to the primary cOECs, the immortalized cOECs were positive to the oviduct markers and the epithelial marker. The group without primary antibody staining was set a negative control. Scale bars: 100 μm.

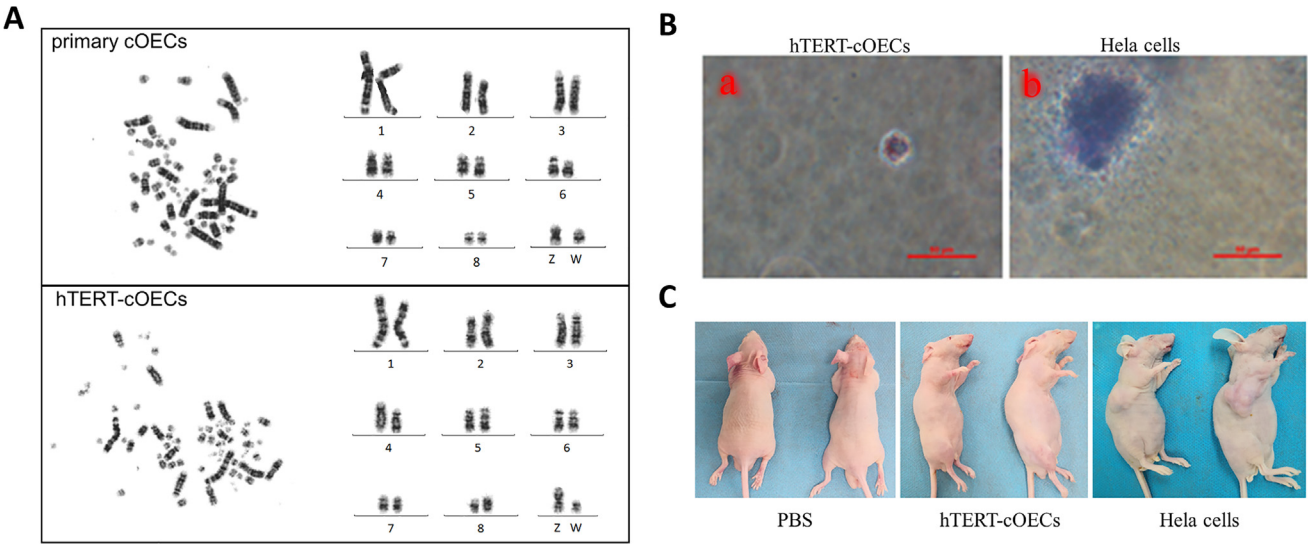

Figure 3. The chromosomal karyotyping and tumorigenicity assay of hTERT-cOECs. (A) Chromosomal karyotyping of primary and hTERT-cOECs at passage 45. Representative images of metaphase cells (left on panels) and macrochromosomes (chromosomes 1−8) and sex chromosomes (Z and W) (right on panels) were presented. G-banded karyotyping revealed that both the primary cOECs and hTERT-cOECs maintained the normal diploid karyotype ($2n = 78$). (B) Typical images of the soft agar cloning assay. As a positive control, Hela cells readily formed colonies in soft agar, whereas the hTERT-cOECs did not. (C) In vivo tumorigenicity assay of hTERT-cOECs. Athymic nude mice were subcutaneously injected with Hela cells (positive control), hTERT-cOECs, and PBS (negative control) and fed for 40 d. The hTERT-cOECs, as well as PBS, did not develop tumors in nude mice, whereas the Hela cells did.

Table 1. sgRNA target sequences and PAMs.

sgRNA names	sgRNA sequence (5′−3′)	PAM
sg1	TACAGTGCTCTGGGTCTTGT	TGG
sg2	TCAGCTTTCTTCTTTTTAAG	GGG
sg3	GTGCTCTGGGTCTTGTTGGA	AGG

sgRNA: single guide RNA; PAM: protospacer adjacent motif.

results are consistent with those achieved in vitro sgRNA cleavage test, where the indel formation rate of sgRNA2 was the highest (75.7%) (Figure 4C). Moreover, DNA sequencing of the PCR amplificon confirmed the sgRNA2-induced indel formation (Figure 4D). All results implied that sgRNA2 is optimal for the following knock-in experiment.

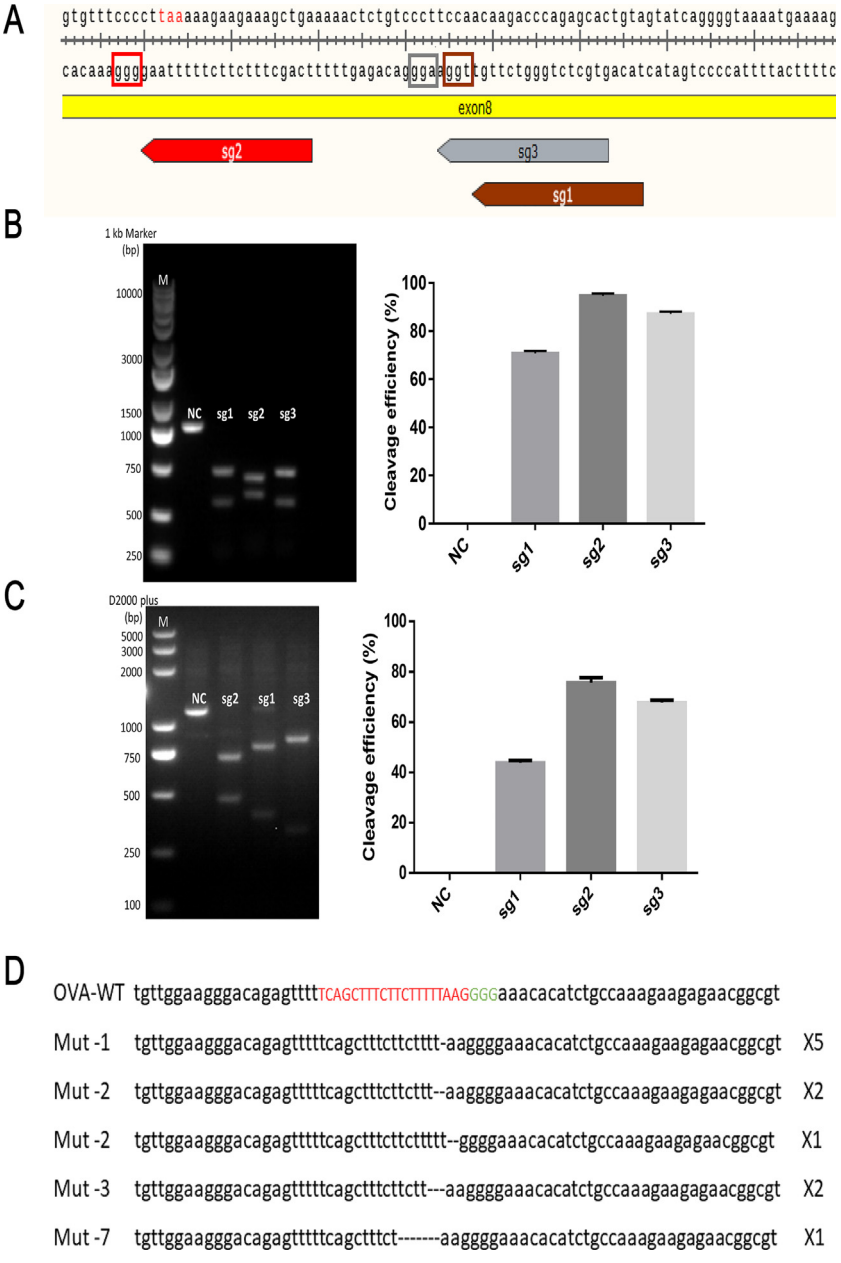

Figure 4. Cleavage efficiency of the selected sgRNA. (A) A schematic illustration of the sgRNA location in the chicken *OVA* locus. The red font TAA indicates the stop codon. The color boxes represent the PAM sequence for each sgRNA. sg1, sg2, and sg3 represent sgRNA1, sgRNA2, and sgRNA3, respectively. (B) In vitro sgRNA cleavage assay. A PCR segment spanning the target region was generated from the chicken genome. It was coincubated with the RNP complex, and the resulting products were resolved on 2% agarose gel. The PCR products presenting as 2 smaller bands implied cleavage. Negative control (NC) is an intact PCR product used as a baseline (left panel). The cleavage efficiency was calculated from the densitometry scanning data (right panel). (C) Cleavage validation of sgRNAs in the hTERT-cOECs through the T7EI assay. The RNP complex was electroporated into the hTERT-cOECs, from which genomic DNA was extracted. The PCR amplicon covering target sites was treated with T7EI. The cleavage products were resolved on 2% agarose gel (left panel). The cleavage efficiency was calculated using densitometry scanning data (right panel). The results derived from both validation methods indicated that sgRNA2 was optimal with the highest cleavage activity. NC, negative control. (D) sgRNA2-induced indels in the hTERT-cOECs were further confirmed through DNA sequencing. The top row indicates the wild-type (WT) *OVA*-sgRNA2 sequence, other rows below represent mutated (Mut) *OVA* sequences. sgRNA2 target sequences are highlighted in red, and the PAM in green. The dotted lines indicate the deleted nucleotides, whose number is denoted as digits (−1 to −7). Multiplied digits (from × 5 to × 1) indicate the number of cell clones with the same mutant.

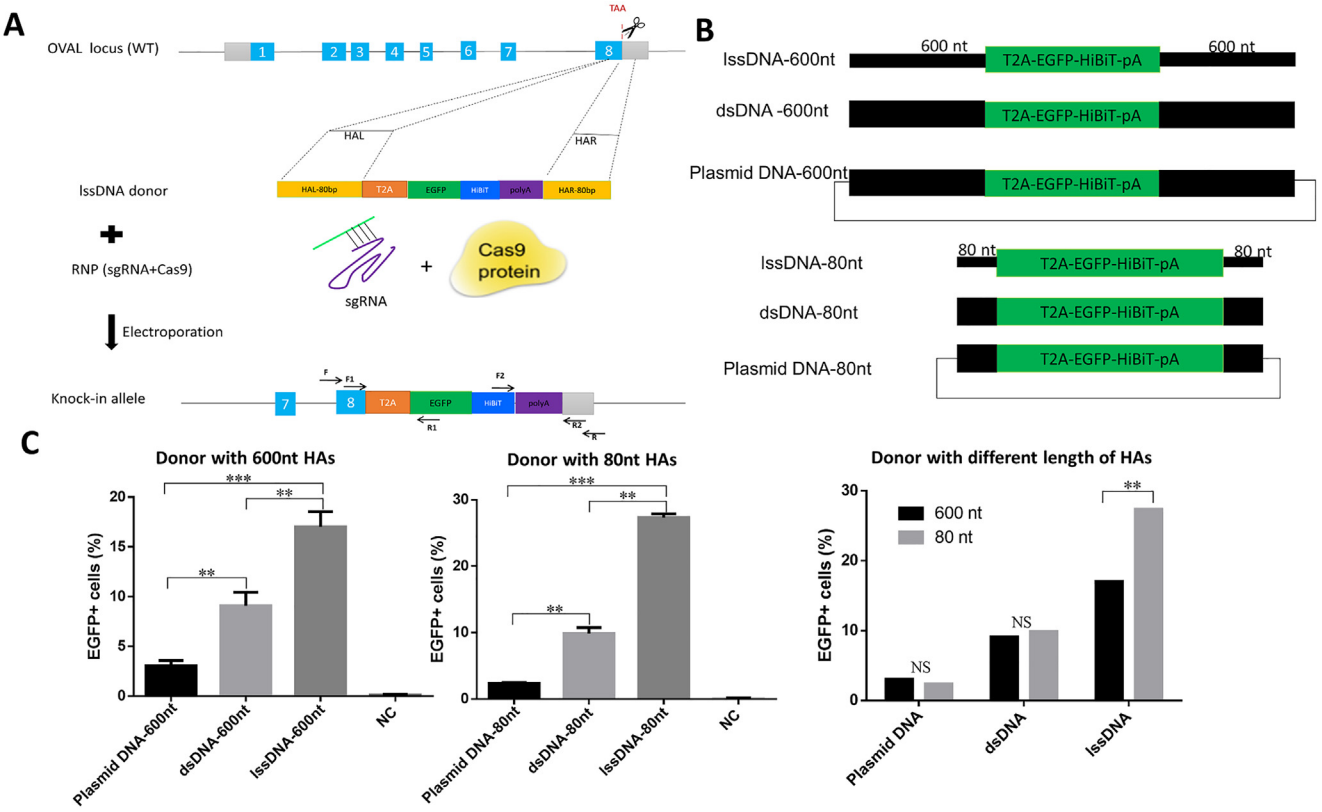

Figure 5. Effects of donor DNA types and length of homologous arms on the *EGFP-HiBiT* KI efficiency. (A) Schematic diagram of KI strategy. A lssDNA donor cassette (*T2A-EGFP-HiBiT-polyA*) flanked with HAs (80 bp each) was electroporated along with the RNP complex to generate the KI allele in the *OVA* locus immediately upstream of the stop codon TAA (in red). Exons are highlighted in numbered boxes (in sky blue); the black full lines between exons indicate introns. WT: wild-type genome sequence; HAL: HA of the left; HAR: HA of the right; F/R, F1/R1, and F2/R2 indicated genotyping primers. (B) Different formats of *EGFP-HiBiT* donors flanked with 600 or 80-bp HAs. (C) Comparison of the *EGFP-HiBiT* KI efficiency using different donors in the hTERT-cOECs. Flow cytometry revealed that the percentage of EGFP+ cells in lssDNA with shorter HAs (80 bp each) was considerably higher than that in the circular (plasmid) and linearized (PCR fragment) donor cassettes with longer HAs (600 bp each).

Easi-CRISPR-Mediated HDR KI Efficiency of EGFP-HiBiT in hTERT-cOECs

Since dsDNA and ssDNA repair templates and the HA length affect the KI efficiency, the KI efficiencies were compared using ssDNA and dsDNA repair templates flanked with 80- or 600-base HAs on each side. The donor DNA plasmid and its PCR amplicon served as the repair dsDNA templates. As illustrated in Figure 5, the percentage of EGFP+ cells using the lssDNA repair template was considerably higher than that using the dsDNA repair templates, and the lssDNA repair template with shorter HAs resulted in a higher percentage of EGFP+ cells than that with longer HAs (27 vs. 17%). Taken together, these results suggest that lssDNA with 80-base HAs is the optimal repair template for *EGFP-HiBiT* KI in the cOECs.

For a reliable genotyping assay, monoclonal EGFP + cell colonies were generated through multiple successive manipulations—FACS sorting, LDM-mediated single cell cloning, and expanding culture (Figure 6A and B). As shown in Figure 6C and D, the EGFP + cell percentage was 27.9% in the KI cell pool, and that reached 78.9 and 97.7% in the FACS-sorted KI cells and in the EGFP+ single cell expanding culture, respectively.

Validation of KI in hTERT-cOECs

Genotyping was performed to confirm the insertion of the *EGFP-HiBIT* donor cassette. The external primers (F/R) were used to amplify the full DNA donor cassette, while the internal primers (F1/R1, F2/R2) were used to amplify 5′ and 3′ junction areas, respectively (Figure 7A). The primer sequences are listed in Supplementary Table S1. Genotyping analysis showed that the KI event occurred in 168 cell colonies. Two of the 168 cell colonies (1%) (colony #19 and #162) were homozygous because only one band (1.8 kb) was detected, and the remaining clones were all monoallelic KI. PCR amplification of 5′ and 3′ junction areas, along with DNA sequencing, confirmed that the donor cassette was knocked in the desired target site (Figure 7B). Furthermore, the HiBiT blotting assay revealed that the expression of the *EGFP-HiBiT* fusion protein was detectable in the KI cells but not in the intact hTERT-cOECs (Figure 7C and D). These results indicated that targeted

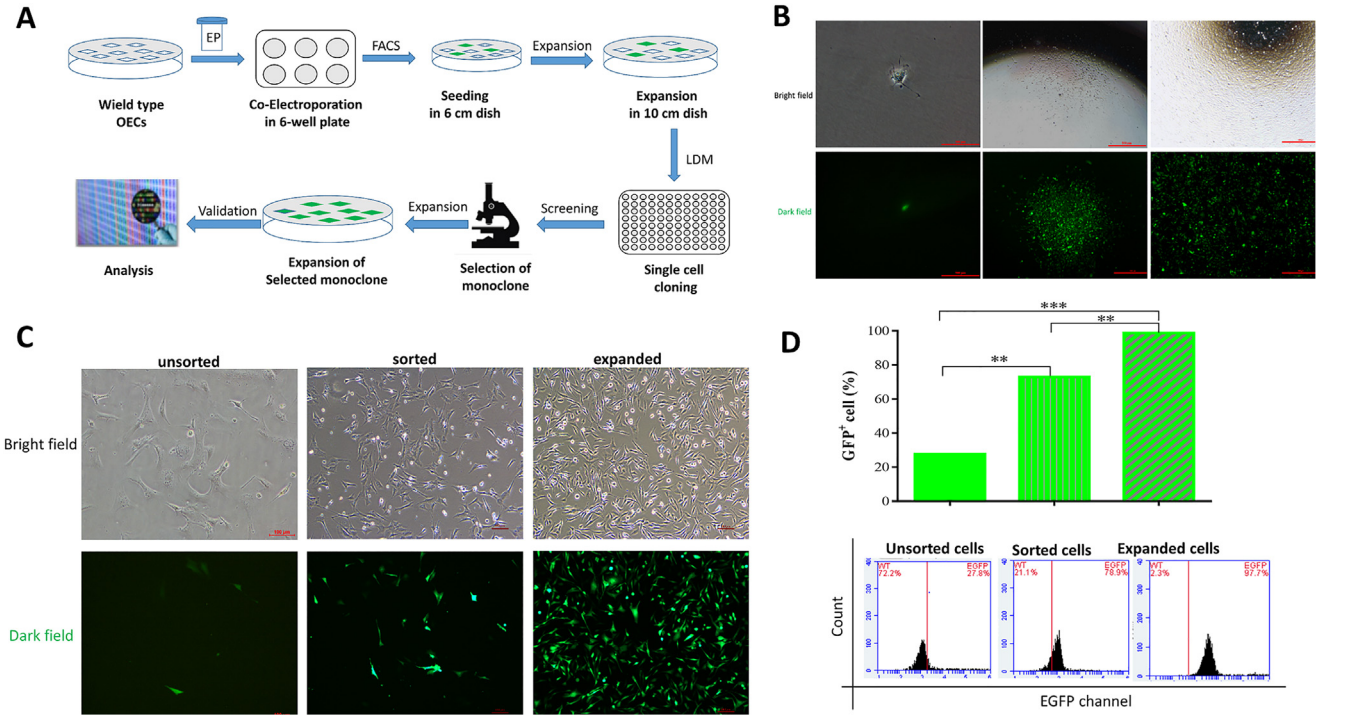

Figure 6. Electroporation-based *EGFP-HiBiT* KI to the *OVA* locus. (A) The workflow for generating fluorescent KI stable cell lines. (B) EGFP + monoclonal cells were screened using the limited dilution method (LDM), and a single cell expanding culture was followed. Scale bar: 500 μm. (C) The representative images of the hTERT-cOECs at 3 different stages: unsorted, sorted, and expanded single cell culture. Scale bars: 100 μm. (D) Percentage of EGFP+ cells were evaluated in the unsorted, sorted, and expanded single cell culture through flow cytometry (bottom panel). The histogram showed that the EGFP+ cell percentage was 27.9% after the delivery and that it reached 97.7% in the expanded single cell culture (top panel).

KI of *EGFP-HiBiT* was successfully achieved using the electroporation-based Easi-CRISPR approach.

Safety Assessment of the Easi-CRISPR KI System in cOECs

As shown in Figure 7C and D, OVA expression was determined in the wild-type (**WT**) and knock-in (**KI**) groups, and the endogenous OVA expression level in the 2 KI cell clones with biallelic insertions was nearly equal to that in the intact hTERT-cOECs. These results suggest that *EGFP-HiBiT* insertion did not repress endogenous OVA expression. To further determine whether Easi-CRISPR-mediated *EGFP-HiBiT* insertion is harmful to the hTERT-cOECs, the proliferation of the KI cells and the intact hTERT-cOECs was comparatively investigated using CCK8. Endogenous OVA expression level of these 2 types of cells was also detected through Western blot and ELISA assays. The CCK8 assay demonstrated that the proliferation of KI cells was comparable to that of the intact hTERT-cOECs (Figure 8A). Furthermore, the ELISA assay (Figure 8B) also illustrated no difference between the KI cells and the intact hTERT-cOECs in the endogenous OVA concentration (6.494 vs. 6.501 pg/cell/d), and these 2 types of cells were similar morphologically. The results implied that the expression level of the endogenous OVA and KI cell proliferation were not affected by transgene integration. Furthermore, 5 predicted potential OTS were evaluated using the T7EI assay. No mutation was detected in these potential OTS (Figure 8C and Table 2), indicating that Easi-CRISPR-mediated KI is efficient and secure in chicken cells and thus can be used in chicken embryos.

DISCUSSION

In this study, the primary cOECs were isolated from young laying hens, and the immortalized cOECs were obtained through hTERT retrovirus infection. The hTERT-cOECs showed the same morphology as the primary cOECs, exhibited stable proliferation, and maintained a normal karyotype. They had no potential for malignant transformation. In addition, the hTERT-cOECs were positive for oviduct markers (OVA, OVM, PGR, ESR1) and epithelial marker (CK18), thus maintaining the features of normal cOECs. Subsequently, Easi-CRISPR components were electroporated to the hTERT-cOECs, and an *EGFP-HiBiT* reporter was inserted into the target site of *OVA*, immediately upstream of the stop codon. Genotyping and DNA sequencing assays revealed that the KI efficiency was 27.9% after electroporation, and this efficiency increased to 97.7% in the single cell expanding culture. More importantly, 2 of the 168 cell clones contained biallelic insertions of *EGFP-HiBiT* cassettes.

Although some attempts have been made to isolate and culture cOECs, some problems remain to be resolved. Jung et al. (2011) first reported the isolation

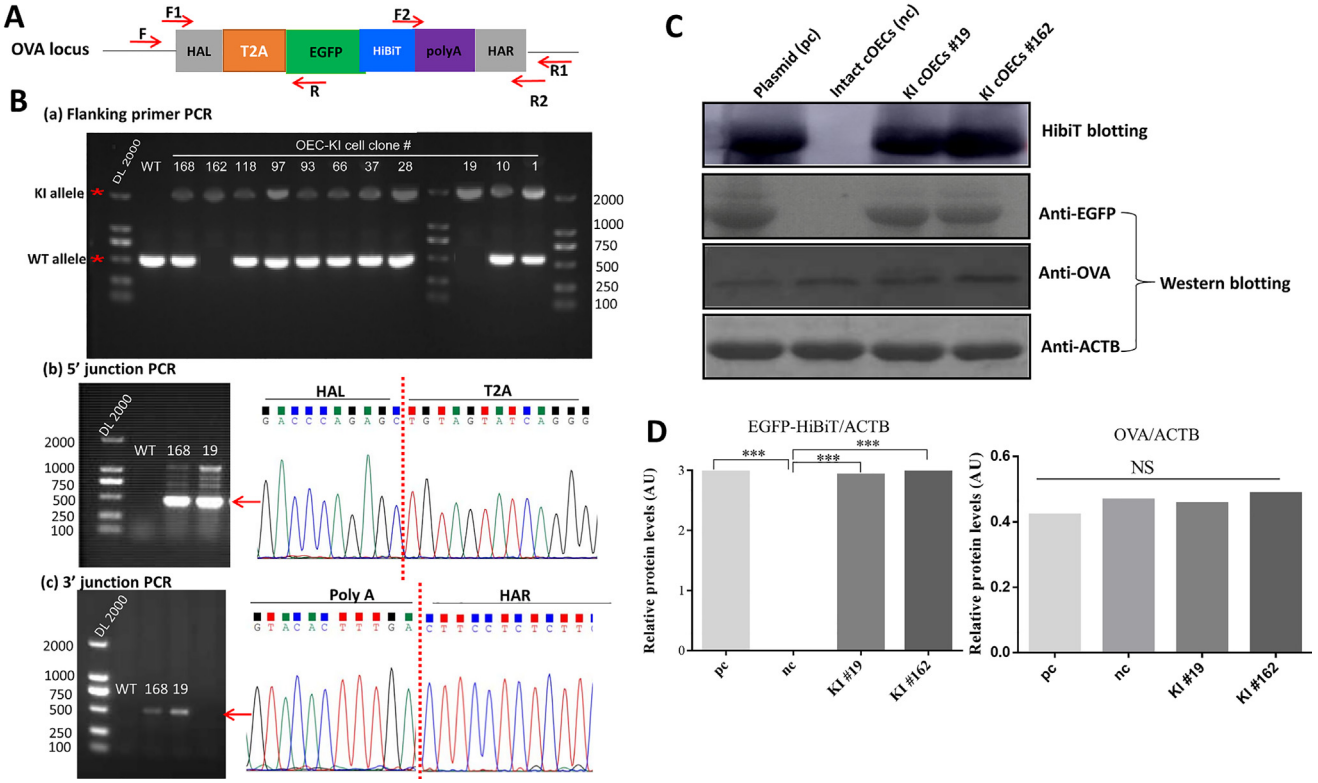

Figure 7. Genotyping KI allele and detection of *EGFP-HiBiT* expression. (A) Locations of 3 pairs of PCR primers for genotyping. The full KI cassette was PCR amplified using flanking primers (F/R); and 5′- and 3′-junction areas around cleavage site were amplified with F1/R1 and F2/R2 primers, respectively. (B) Genotyping gel images. (a) Flanking primer PCR. The gel showed that genomic PCR amplification of 2 cell clones (#162 and #19) with F/R primers generated only 1 mutant amplicon, indicating that they were biallelic insertions, and other cell clones were monoallelic insertions; (b) 5′-junction PCR and sequence chromatograms (on the right); (c) 3′-junction PCR and sequence chromatograms (on the right). (C) Expression detection of HiBiT-tagged *EGFP* and *OVA* through HiBiT blotting and Western blotting. The edited cell clones (#162 and #19) were set as the test group, the hTERT-cOECs transfected with a plasmid encoding *EGFP-HiBiT* (pcDNA3.1/*EGFP-HiBiT*) served as a positive control (pc), and intact hTERT-cOECs served as a negative control (nc). HiBiT blotting showed HiBiT-tagged *EGFP* expression in the test and positive control groups, but not in the negative control group (top panel). Western blotting showed OVA expression in all of groups, and EGFP expression in the test and positive group. ACTB served as an internal control. (D) Histograms based on densitometry scanning data derived from HiBiT and Western blotting. Densitometry scanning data were derived from 3 independent blotting experiments, and relative EGFP-HiBiT/OVA expression was quantified as the ratio of EGFP-HiBiT/OVA to ACTB densitometry scanning data. The relative EGFP-HiBiT expression level in the 2 cell clones with biallelic insertions was nearly equal to that in the plasmid-transfected hTERT-cOECs, and no difference was observed in the relative OVA expression among the 3 groups, suggesting that endogenous OVA expression was not repressed by *EGFP-HiBiT* insertion. NS: no significance.

and culture of cOECs, and Kasperczyk et al. (2012) tested different factors affecting cOEC primary cultures, such as the origin of isolated cells, the oviduct tissue dissociation procedure, tissue digestion times, culture plate coating, growth media, incubation temperature, and different cell seeding numbers. However, another problem should be addressed: the inner surface of oviducts is covered by a thick mucus layer, which weakens enzymatic digestion, hindering cOEC isolation. As a strong reducing agent, DTT can break disulfide bonds in polymers and has been used as a mucolytic agent for homogenizing sputum to facilitate cytological experiments, recover cells, and detect mediators (Ryu et al., 2017). Because Dispase II has a moderate proteolytic function, it has been used to isolate volatile primary cells from animal tissues, for instance, mouse alveolar epithelial cells (Hansen et al., 2014), swine gastric epithelial cells (Bautista-Amorocho et al., 2021), mouse esophageal stem cells (Maghsoudlou et al., 2014), and mouse airway brush cells (Ualiyeva and Bankova, 2022). Therefore, in this study, 1% DTT solution was used to remove the thick mucus layer prior to mechanical dissociation and digestion of the oviduct mucosal tissues with 0.25% Dispase II. Finally, the primary cOECs were obtained along with the maximal remove of the fibroblastic contaminating cells by using the DAM, indicating that the cell isolation procedure was efficient.

The cleavage efficiency of sgRNAs, length of insertions, and donor formats are factors crucial for a successful KI experiment. The CRISPR/Cas9-mediated KI efficiency heavily depended on the cleavage efficiencies of sgRNAs. Using the online software CHOPCHOP, multiple sgRNAs with higher scores were chosen and their cutting efficiencies were validated before of the KI experiment. Here, we tested the efficiencies of 3 sgRNAs against the *OVA* gene and found sgRNA2 was optimal with the highest cleavage efficiency (94.6%) (Figure 4B and C). Moreover, the integration site of the donor cassette was in the proximity (2 bp) of the DSBs when sgRNA2 was adopted, thereby meeting the requirement for vicinity (≤7 bp) in the cleavage site (Liang et al., 2017). Furthermore, the donor type and HA length

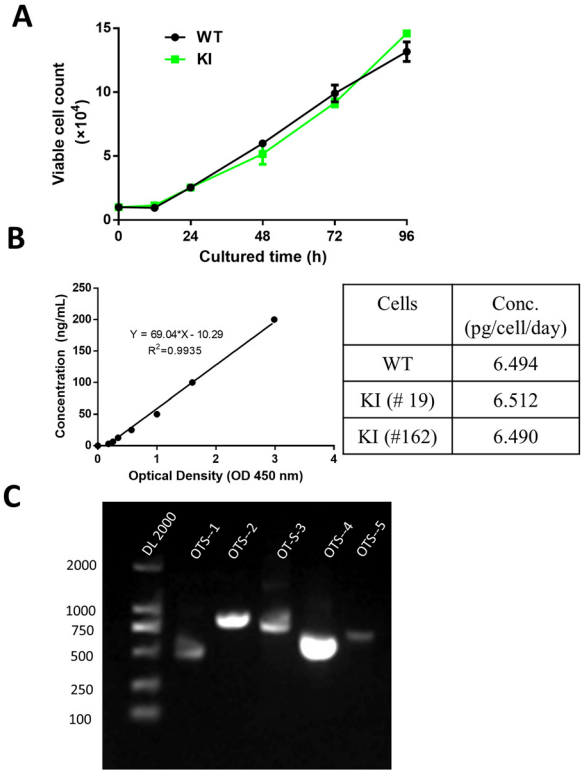

Figure 8. Safety assessment of the Easi-CRISPR system in cOECs. (A) CCK-8 was used to test the proliferation of KI cells. No significant difference in proliferation was observed between the edited hTERT-cOECs (KI) and the intact hTERT-cOECs (WT). (B) Detection of the endogenous OVA protein in KI cells and intact hTERT-cOECs through ELISA. A commercially available chicken egg albumin served as baseline. The content of endogenous OVA protein in the KI cells was calculated according to the manufacturer's instruction. As indicated in the right panel, OVA concentrations in the KI cells were comparable to those in the intact hTERT-cOECs. (C) Analysis for off-target effects. Using an online software, 5 potential OTS were predicted, and genomic PCR was performed to amplify individual segments around each site with the corresponding primer pairs. The resulting amplicons were analyzed using the T7EI assay. As shown in the gel image, no off-target effect was detected.

affect the KI efficiency. Two research groups reported that the single-strand oligodeoxynucleotide (**ssODN**) and PCR segment with shorter HAs outperformed the dsDNA plasmid donor with longer HAs in the HDR-mediated small DNA KI (≤200 bp) (Paquet et al., 2016; Paix et al., 2017). Here, even if the transgene cassette was 1.1 kb in size, much longer than the ssODN used in the 2 aforementioned studies, irrespective of Cas9/sgRNA delivery, a similar result was obtained—the KI efficiency for the lssDNA with shorter HAs (80 bp each) was considerably higher than that for the circular (plasmid) and linearized (PCR fragment) transgene cassettes with longer HAs (600 bp each) (Figure 5). This is also in line with the findings in chicken PGC cells (Idoko-Akoh et al., 2018), Xenopus eggs (Nakayama et al., 2022), and mouse embryos (Codner et al., 2018; Miura et al., 2018; Bennett et al., 2021).

The formats of Cas9, DNA, mRNA, or protein also determine the gene editing efficiency. Plasmid DNA transfection leads to Cas9 expression for a longer period in cells, increasing the chance of off-target effects (Yip, 2020). Although Cas9 mRNA transfection can initiate gene editing more quickly than plasmid DNA, mRNA tends to be readily degraded by RNases (Lin et al., 2022). However, Cas9 protein (RNP complex) transfection is superior to plasmid DNA and mRNA transfection because the RNP complex bypasses transcription and translation, and thus, gene editing is quickly initiated, thereby leading to the immediate degradation of the complex in the target cells. Therefore, Cas9-RNP delivery contributes to achieving a higher editing efficiency, reducing off-target effects, rapidly screening sgRNAs with higher cutting efficiency in vitro, and diminishing immunogenicity (Yip, 2020; Tyumentseva et al., 2021). Miura et al. (2018) and Quadros et al. (2017) developed the Easi-CRISPR-mediated KI approach by combining Cas9 RNP and the lssDNA donor. Injection of RNP plus the ssDNA donor to mouse zygotes leads to a typical editing efficiency of 30 to 60% in 13 loci, especially at least one GE founder with biallelic insertions could be generated in a single generation by injecting an average of 50 zygotes. The KI allele could be detected in all live offspring, indicating that Easi-CRISPR is highly efficient. In addition, a ssDNA donor was advantageous over a dsDNA donor, because the editing efficiency and embryonic viability with the ssDNA donor were 2.5 and 2.4 times higher than with the dsDNA donor, respectively.

The CRISPR-RNP delivery strategy should also be considered in gene editing. Although physical injection and commercially available transfection reagents (e.g., Lipofectamine CRISPRMAX) are used to deliver CRISPR-RNPs to cells or zygotes, electroporation is a promising physical delivery method. Electroporation opens nanopores transiently in the cell membrane through electric stimulation and allows CRISPR

Table 2. Analysis of potential off-target sites.

Potential off-target sites	Genomic location	Sequence	Indel
OVA-sgRNA2	chr2:67683097	TCAGCTTTCTTCTTTTTAAG**GGG**	-
OTS-1	chr1:137184080	TCtGCTcTCTTCTTTTTAtG**TGG**	No
OTS-2	chr2:107006660	cCaGCTTTCTTCaTTTTAAG**TGG**	No
OTS-3	chr20:3937312	TtgaCTTTCTTCTTTTTAAG**AGG**	No
OTS-4	chr3:70415544	TCAGaTTTCTTCTTaaTAAG**GGG**	No
OTS-5	chr4:17364358	TCctCTTTCTTtTTTTTAAG**AGG**	No

Five potential OTS were selected, and the off-target effects were verified through the T7EI assay and DNA sequencing. Bold letters indicate PAM sequences. Lowercase letters indicate mismatches with the original OVA sgRNA2 sequences in the nucleotide. The last column shows the detected indels.

components to enter cells. Given that electroporation can be used to efficiently transfer CRISPR reagents into many types of cells, it is applicable for in vitro and ex vivo gene editing (Zhang et al., 2021). By contrast, conventional transfection methods are hampered in difficult-to-transfect cells, including stem cells and primary cells (Yip, 2020). However, electroporation is usually associated with high levels of cell death (Tyumentseva et al., 2021). Chen et al. (2016) used an electroporation-based method—CRISPR RNP electroporation of zygotes (**CRISPR-EZ**) to transport Cas9-RNP complexes into mouse zygotes. Consequently, the delivery efficiency was up to 100% under the optimized conditions (30 V, 6 pulses, 3 ms). Furthermore, CRISPR-EZ is scalable for robust gene editing items, for example, indel mutation, exon deletion, point mutation, and small ssODN insertions. Importantly, a 100% biallelic KO and a 62.5% biallelic KI allele of *tyrosinase* gene were detected in 2 inbreed mouse strains exhibiting minimal impact on embryo viability. Remarkably, the editing efficiency was 3-fold higher using CRISPR-EZ than using microinjections. The results indicated that electroporation-based Cas9/sgRNA RNP delivery is more efficient than microinjection-based delivery. Therefore, we chose electroporation-based Easi-CRISPR for *EGFP-HiBiT* KI in hTERT-cOECs.

Editing efficacy and its specificity, survival rate of target cells/embryos after delivery, and scalabilities of the transfer process are criteria for gene editing and should be followed and evaluated (Tyumentseva et al., 2021). In our electroporation-based Easi-CRISPR KI experiment, the *EGFP-HiBiT* KI efficiency was close to 30% in hTERT-cOECs, and more importantly, biallelic insertions were determined in 2 cell clones. The editing efficiency was moderate, lower than that in mouse embryos for which CRISPR-EZ was used (Chen et al., 2016; Sentmanat et al., 2022) and higher than that in human T cells (Schumann et al., 2015). A possible explanation is that, in our study, Cas9-to-sgRNA ratios were established according to the manufacturer's instruction, and electroporation conditions (160 V, single pulse, 5 ms) for the hTERT-cOECs were determined empirically on the basis of a previous work of our group (Liu et al., 2022). These 2 factors remain to be extensively optimized. Moreover, both the T7EI assay and DNA sequencing showed that off-target effects were not detected in the *OVA* gene, indicating that *EGFP-HiBiT* insertion is specific. Furthermore, no significant difference in proliferation was observed between the edited hTERT-cOECs and the intact hTERT-cOECs (Figure 8A), thereby illustrating that electroporation-based Easi-CRISPR has less impact on the survival rate of the target cells after electroporation. Although the scalabilities of the editing approach were not performed in our study, it has been investigated in 13 loci of the mouse genome by Quadros et al. (2017) and Miura et al. (2018), and in different editing schemes including indel mutation, exon deletion, point mutation, and small insertions in mice by Chen et al. (2016) and Sentmanat et al. (2022). Finally, HiBiT-tagged EGFP expression was simply and quickly verified in the edited cells through the HiBiT blotting technique (Figure 7C). This method was more superior to standard antibody-based Western blotting protocols, as it is simple, time saving, and beneficial for the quick screening of transient transfections or CRISPR KIs (Madsen and Semple, 2019; Boursier et al., 2020; White et al., 2020). Generally, electroporation-mediated Easi-CRISPR is highly effective in chicken cOECs, but its effectiveness in chicken embryos needs to be explored. Of note, cellular enrichment through drug selection was conducted here for reliable genotyping of target cells. However, this manipulation could not be performed in an ex vivo KI experiment conducted in chicken embryos. Therefore, electroporation-based Easi-CRISPR needs to be improved ex vivo. The related work is currently being conducted in our laboratory. This includes ex vivo validation of the sgRNA efficiency, optimization of Cas9-to-sgRNA ratios, refining of electroporation conditions, analysis of the *EGFP-HiBiT* KI efficiency in developing embryos, and screening of G0 founders. Findings will be reported in a future publication.

Further development of electroporation-based Easi-CRISPR techniques will foster rapid generation of GE birds. In mammals, CRISPR components are usually delivered to a single-cell zygote through microinjection, and the edited embryos at the blastula stage are transferred to the oviducts of surrogates. However, such embryo transplantation could not be performed in avian species owing to its unique reproductive system. During in vitro editing and enrichment, the cultured PGCs were transferred to embryonic blood vessels through microinjection (Oishi et al., 2018; Mukae et al., 2020) or direct microinjection of editing reagents to embryonic blood vessels (Tyack et al., 2013) is the current method for gene editing in birds. However, the editing efficiencies are suboptimal, and at least 2 generations are required to generate a bird carrying biallelic insertions of DNA donor cassettes (Cooper et al., 2018). By contrast, sperm transfection-assisted gene editing (**STAGE**) can simplify gene editing in birds and shorten the time line for breeding GE birds. For example, in Cooper et al.'s work (ʻCooper et al., 2017), Cas9 mRNA and sgRNA were delivered to chicken sperm through lipofectamine transfection, and the transfected sperm were artificially inseminated in hens. Consequently, homozygous GE chickens were generated in a single generation; this is in accordance with using microinjection- and electroporation-based Easi-CRISPR in mouse embryos (Chen et al., 2016; Quadros et al., 2017; Miura et al., 2018), as well as consistent with our results in the hTERT-cOECs. Of note, a red fluorescent protein (***RFP***) reporter KI experiment has been conducted in our laboratory through electroporation-based Easi-CRISPR plus STAGE. Chicken Pax7 (intron 1) was selected as the targeting locus. Easi-CRISPR components were delivered to the nerve tube of chicken embryos at embryonic day (**ED**) 2.5 through microinjection. The embryos were electroporated immediately. *RFP* expression and the *RFP* KI efficiency was confirmed in the developing embryos through microscopy and genotyping. Subsequently, the

same components of Easi-CRISPR were electroporated to rooster sperm, which was artificially inseminated in hens. *RFP* expression was detected in the brain, nerve tube, and muscles of the developing embryos and hatched chicks, and *RFP* integration was also verified through genotyping (unpublished data). Therefore, one can reasonably foresee that homozygous GE chickens could be generated in a single generation if electroporation-based Easi-CRISPR is combined with STAGE. This is meaningful for poultry breeding and production.

In conclusion, our established immortalized cOECs are promising as they can serve as an in vitro gene editing model for investigating the secreting function of cOECs, and this electroporation-based Easi-CRISPR strategy will contribute to the generation of avian bioreactors and other GE birds.

ACKNOWLEDGMENTS

This research was financially supported by the National Natural Science Foundation of China (32060738; 31660653), the Natural Science Foundation of Guangxi Province (2018GXNSFDA281026), and the Science and Technology R & D Project of Guangxi Province (GuikeAB16380098). The authors would like to thank all the reviewers who participated in the review, as well as MJEditor (www.mjeditor.com) for providing English editing services during the preparation of this manuscript.

DISCLOSURES

The authors declare that they have no known competing financial interests or personal relationships that could have appeared to influence the work reported in the present study.

SUPPLEMENTARY MATERIALS

Supplementary material associated with this article can be found in the online version at doi:10.1016/j.psj.2023.103112.

REFERENCES

Bahrami, S., A. Amiri-Yekta, A. Daneshipour, S. H. Jazayeri, P. E. Mozdziak, M. H. Sanati, and H. Gourabi. 2020. Designing a transgenic chicken: applying new approaches toward a promising bioreactor. Cell J. 22:133–139.

Barman, A., B. Deb, and S. Chakraborty. 2020. A glance at genome editing with CRISPR-Cas9 technology. Curr. Genet. 66:447–462.

Bautista-Amorocho, H., J. A. Silva-Sayago, D. A. Goyeneche-Patino, T. L. Pérez-Cala, F. Macías-Gómez, J. C. Arango-Viana, and A. Martínez. 2021. A novel method for isolation and culture of primary swine gastric epithelial cells. BMC Mol. Cell Biol. 22:1.

Bennett, H., E. Aguilar-Martinez, and A. D. Adamson. 2021. CRISPR-mediated knock-in in the mouse embryo using long single stranded DNA donors synthesised by biotinylated PCR. Methods 191:3–14.

Bertolini, L. R., H. Meade, C. R. Lazzarotto, L. T. Martins, K. C. Tavares, M. Bertolini, and J. D. Murray. 2016. The transgenic animal platform for biopharmaceutical production. Transgenic Res. 25:329–343.

Boursier, M. E., S. Levin, K. Zimmerman, T. Machleidt, R. Hurst, B. L. Butler, C. T. Eggers, T. A. Kirkland, K. V. Wood, and R. Friedman Ohana. 2020. The luminescent HiBiT peptide enables selective quantitation of G protein-coupled receptor ligand engagement and internalization in living cells. J. Biol. Chem. 295:5124–5135.

Cao, D., H. Wu, Q. Li, Y. Sun, T. Liu, J. Fei, Y. Zhao, S. Wu, X. Hu, and N. Li. 2015. Expression of recombinant human lysozyme in egg whites of transgenic hens. PLoS One 10:e0118626.

Carneiro, I. S., J. N. R. Menezes, J. A. Maia, A. M. Miranda, V. B. S. Oliveira, J. D. Murray, E. A. Maga, M. Bertolini, and L. R. Bertolini. 2018. Milk from transgenic goat expressing human lysozyme for recovery and treatment of gastrointestinal pathogens. Eur. J. Pharm. Sci. 112:79–86.

Chen, S., B. Lee, A. Y. Lee, A. J. Modzelewski, and L. He. 2016. Highly efficient mouse genome editing by CRISPR ribonucleoprotein electroporation of zygotes. J. Biol. Chem. 291:14457–14467.

Codner, G. F., J. Mianné, A. Caulder, J. Loeffler, R. Fell, R. King, A. J. Allan, M. Mackenzie, F. J. Pike, C. V. McCabe, S. Christou, S. Joynson, M. Hutchison, M. E. Stewart, S. Kumar, M. M. Simon, L. Agius, Q. M. Anstee, K. E. Volynski, D. M. Kullmann, S. Wells, and L. Teboul. 2018. Application of long single-stranded DNA donors in genome editing: generation and validation of mouse mutants. BMC Biol. 16:70.

Cooper, C. A., A. Challagulla, K. A. Jenkins, T. G. Wise, T. E. O'Neil, K. R. Morris, M. L. Tizard, and T. J. Doran. 2017. Generation of gene edited birds in one generation using sperm transfection assisted gene editing (STAGE). Transgenic Res. 26:331–347.

Cooper, C. A., T. J. Doran, A. Challagulla, M. L. V. Tizard, and K. A. Jenkins. 2018. Innovative approaches to genome editing in avian species. J. Anim. Sci. Biotechnol. 9:15.

Dimitrov, L., D. Pedersen, K. H. Ching, H. Yi, E. J. Collarini, S. Izquierdo, M. C. van de Lavoir, and P. A. Leighton. 2016. Germline gene editing in chickens by efficient CRISPR-mediated homologous recombination in primordial germ cells. PLoS One 11:e0154303.

Ezaki, R., K. Ichikawa, M. Matsuzaki, and H. Horiuchi. 2022. Targeted knock-in of a fluorescent protein gene into the chicken vasa homolog locus of chicken primordial germ cells using CRIS-PITCh method. J. Poult. Sci. 59:182–190.

Farzaneh, M., S. N. Hassani, P. Mozdziak, and H. Baharvand. 2017. Avian embryos and related cell lines: a convenient platform for recombinant proteins and vaccine production. Biotechnol. J. 12:e1600598.

Gallagher, D. N., and J. E. Haber. 2021. Single-strand template repair: key insights to increase the efficiency of gene editing. Curr. Genet. 67:747–753.

Hagihara, Y., Y. Okuzaki, K. Matsubayashi, H. Kaneoka, T. Suzuki, S. Iijima, and K. I. Nishijima. 2020. Primordial germ cell-specific expression of eGFP in transgenic chickens. Genesis 58:e23388.

Hansen, T., A. Chougule, and J. Borlak. 2014. Isolation and cultivation of metabolically competent alveolar epithelial cells from A/J mice. Toxicol. In Vitro 28:812–821.

Hay, A. N., K. Farrell, C. M. Leeth, and K. Lee. 2022. Use of genome editing techniques to produce transgenic farm animals. Adv. Exp. Med. Biol. 1354:279–297.

Herron, L. R., C. Pridans, M. L. Turnbull, N. Smith, S. Lillico, A. Sherman, H. J. Gilhooley, M. Wear, D. Kurian, G. Papadakos, P. Digard, D. A. Hume, A. C. Gill, and H. M. Sang. 2018. A chicken bioreactor for efficient production of functional cytokines. BMC Biotechnol. 18:82.

Idoko-Akoh, A., L. Taylor, H. M. Sang, and M. J. McGrew. 2018. High fidelity CRISPR/Cas9 increases precise monoallelic and biallelic editing events in primordial germ cells. Sci. Rep. 8:15126.

Jung, J. G., T. S. Park, J. N. Kim, B. K. Han, S. D. Lee, G. Song, and J. Y. Han. 2011. Characterization and application of oviductal epithelial cells in vitro in Gallus domesticus. Biol. Reprod. 85:798–807.

Kasperczyk, K., A. Bajek, R. Joachimiak, K. Walasik, A. Marszalek, T. Drewa, and M. Bednarczyk. 2012. In vitro optimization of the Gallus domesticus oviduct epithelial cells culture. Theriogenology 77:1834–1845.

Kerekes, A., O. I. Hoffmann, G. Iski, N. Lipták, E. Gócza, W. A. Kues, Z. Bősze, and L. Hiripi. 2017. Secretion of a

recombinant protein without a signal peptide by the exocrine glands of transgenic rabbits. PLoS One 12:e0187214.
Khalil, A. M. 2020. The genome editing revolution: review. J. Genet. Eng. Biotechnol. 18:68.
Kling, J. 2009. First US approval for a transgenic animal drug. Nat. Biotechnol. 27:302–304.
Kwon, M. S., B. C. Koo, D. Kim, Y. H. Nam, X. S. Cui, N. H. Kim, and T. Kim. 2018. Generation of transgenic chickens expressing the human erythropoietin (hEPO) gene in an oviduct-specific manner: production of transgenic chicken eggs containing human erythropoietin in egg whites. PLoS One 13:e0194721.
Lee, S. Y., J. H. Han, E. K. Lee, Y. K. Kim, S. A. Hwang, S. H. Lee, M. Kim, G. Y. Cho, J. H. Hwang, S. J. Kim, J. G. Yoo, S. K. Cho, K. J. Lee, and W. K. Cho. 2020. Structural and functional characterization of recombinant human growth hormone isolated from transgenic pig milk. PLoS One 15:e0236788.
Liang, X., J. Potter, S. Kumar, N. Ravinder, and J. D. Chesnut. 2017. Enhanced CRISPR/Cas9-mediated precise genome editing by improved design and delivery of gRNA, Cas9 nuclease, and donor DNA. J. Biotechnol. 241:136–146.
Lillico, S. G., M. J. McGrew, A. Sherman, and H. M. Sang. 2005. Transgenic chickens as bioreactors for protein-based drugs. Drug Discov. Today 10:191–196.
Lillico, S. G., A. Sherman, M. J. McGrew, C. D. Robertson, J. Smith, C. Haslam, P. Barnard, P. A. Radcliffe, K. A. Mitrophanous, E. A. Elliot, and H. M. Sang. 2007. Oviduct-specific expression of two therapeutic proteins in transgenic hens. Proc. Natl. Acad. Sci. USA 104:1771–1776.
Lin, Y., E. Wagner, and U. Lächelt. 2022. Non-viral delivery of the CRISPR/Cas system: DNA versus RNA versus RNP. Biomater. Sci. 10:1166–1192.
Liu, T., H. Wu, D. Cao, Q. Li, Y. Zhang, N. Li, and X. Hu. 2015. Oviduct-specific expression of human neutrophil defensin 4 in lentivirally generated transgenic chickens. PLoS One 10:e0127922.
Liu, L., J. Zhang, T. Teng, Y. Yang, W. Zhang, W. Wu, G. Li, and X. Zheng. 2022. Electroporation of SUMO-His-Cre protein triggers a specific recombinase-mediated cassette exchange in HEK 293T cells. Protein Exp. Purif. 198:106128.
Luo, Y., L. Lin, L. Bolund, and C. B. Sørensen. 2014. Efficient construction of rAAV-based gene targeting vectors by Golden Gate cloning. BioTechniques 56:263–268.
Madsen, R. R., and R. K. Semple. 2019. Luminescent peptide tagging enables efficient screening for CRISPR-mediated knock-in in human induced pluripotent stem cells. Wellcome Open Res. 4:37.
Maghsoudlou, P., D. Ditchfield, D. H. Klepacka, P. Shangaris, L. Urbani, S. P. Loukogeorgakis, S. Eaton, and P. De Coppi. 2014. Isolation of esophageal stem cells with potential for therapy. Pediatr. Surg. Int. 30:1249–1256.
Miura, H., R. M. Quadros, C. B. Gurumurthy, and M. Ohtsuka. 2018. Easi-CRISPR for creating knock-in and conditional knockout mouse models using long ssDNA donors. Nat. Protoc. 13:195–215.
Mukae, T., S. Okumura, T. Watanobe, K. Yoshii, T. Tagami, and I. Oishi. 2020. Production of recombinant monoclonal antibodies in the egg white of gene-targeted transgenic chickens. Genes (Basel) 12:38.
Nakayama, T., R. M. Grainger, and S. W. Cha. 2022. Homology-directed repair by CRISPR-Cas9 mutagenesis in xenopus using long single-stranded donor DNA templates via simple microinjection of embryos. Cold Spring Harb. Protoc. 2022:606–615.
Oishi, I., K. Yoshii, D. Miyahara, and T. Tagami. 2018. Efficient production of human interferon beta in the white of eggs from ovalbumin gene-targeted hens. Sci. Rep. 8:10203.
Paix, A., A. Folkmann, D. H. Goldman, H. Kulaga, M. J. Grzelak, D. Rasoloson, S. Paidemarry, R. Green, R. R. Reed, and G. Seydoux. 2017. Precision genome editing using synthesis-dependent repair of Cas9-induced DNA breaks. Proc. Natl. Acad. Sci. U. S. A. 114:E10745–E10754.
Paquet, D., D. Kwart, A. Chen, A. Sproul, S. Jacob, S. Teo, K. M. Olsen, A. Gregg, S. Noggle, and M. Tessier-Lavigne. 2016. Efficient introduction of specific homozygous and heterozygous mutations using CRISPR/Cas9. Nature 533:125–129.
Petitte, J. N., and P. E. Mozdziak. 2007. The incredible, edible, and therapeutic egg. Proc. Natl. Acad. Sci. U. S. A. 104:1739–1740.
Quadros, R. M., H. Miura, D. W. Harms, H. Akatsuka, T. Sato, T. Aida, R. Redder, G. P. Richardson, Y. Inagaki, D. Sakai, S. M. Buckley, P. Seshacharyulu, S. K. Batra, M. A. Behlke, S. A. Zeiner, A. M. Jacobi, Y. Izu, W. B. Thoreson, L. D. Urness, S. L. Mansour, M. Ohtsuka, and C. B. Gurumurthy. 2017. Easi-CRISPR: a robust method for one-step generation of mice carrying conditional and insertion alleles using long ssDNA donors and CRISPR ribonucleoproteins. Genome Biol. 18:92.
Ranawakage, D. C., K. Okada, K. Sugio, Y. Kawaguchi, Y. Kuninobu-Bonkohara, T. Takada, and Y. Kamachi. 2020. Efficient CRISPR-Cas9-mediated knock-in of composite tags in zebrafish using long ssDNA as a donor. Front. Cell Dev. Biol. 8:598634.
Ryu, H., K. Choi, Y. Qu, T. Kwon, J. S. Lee, and J. Han. 2017. Patient-derived airway secretion dissociation technique to isolate and concentrate immune cells using closed-loop inertial microfluidics. Anal. Chem. 89:5549–5556.
Sampson, T. R., and D. S. Weiss. 2014. Exploiting CRISPR/Cas systems for biotechnology. Bioessays 36:34–38.
Schumann, K., S. Lin, E. Boyer, D. R. Simeonov, M. Subramaniam, R. E. Gate, G. E. Haliburton, C. J. Ye, J. A. Bluestone, J. A. Doudna, and A. Marson. 2015. Generation of knock-in primary human T cells using Cas9 ribonucleoproteins. Proc. Natl. Acad. Sci. U. S. A. 112:10437–10442.
Sentmanat, M. F., J. M. White, E. Kouranova, and X. Cui. 2022. Highly reliable creation of floxed alleles by electroporating single-cell embryos. BMC Biol. 20:31.
Sheridan, C. 2016. FDA approves 'farmaceutical' drug from transgenic chickens. Nat. Biotechnol. 34:117–119.
Shola, D. T. N., C. Yang, C. Han, R. Norinsky, and R. D. Peraza. 2021. Generation of mouse model (KI and CKO) via Easi-CRISPR. Methods Mol. Biol. 2224:1–27.
Tyack, S. G., K. A. Jenkins, T. E. O'Neil, T. G. Wise, K. R. Morris, M. P. Bruce, S. McLeod, A. J. Wade, J. McKay, R. J. Moore, K. A. Schat, J. W. Lowenthal, and T. J. Doran. 2013. A new method for producing transgenic birds via direct in vivo transfection of primordial germ cells. Transgenic Res. 22:1257–1264.
Tyumentseva, M. A., A. I. Tyumentsev, and V. G. Akimkin. 2021. Protocol for assessment of the efficiency of CRISPR/Cas RNP delivery to different types of target cells. PLoS One 16:e0259812.
Ualiyeva, S., and L. G. Bankova. 2022. Isolation, ex vivo culture, and stimulation of tracheal and nasal chemosensory cells. Methods Mol. Biol. 2506:151–165.
White, C. W., B. Caspar, H. K. Vanyai, K. D. G. Pfleger, and S. J. Hill. 2020. CRISPR-Mediated protein tagging with nanoluciferase to investigate native chemokine receptor function and conformational changes. Cell Chem. Biol. 27:499–510 e497.
Yamamoto, Y., and S. A. Gerbi. 2018. Making ends meet: targeted integration of DNA fragments by genome editing. Chromosoma 127:405–420.
Yang, H., B. R. Lee, H. C. Lee, S. K. Jung, J. Y. Kim, J. No, S. Shanmugam, Y. J. Jo, H. Lee, S. Hwang, and S. J. Byun. 2021. Isolation and characterization of cultured chicken oviduct epithelial cells and in vitro validation of constructed ovalbumin promoter in these cells. Anim. Biosci. 34:1321–1330.
Yip, B. H. 2020. Recent advances in CRISPR/Cas9 delivery strategies. Biomolecules 10:839.
Zeng, F., Z. Li, Q. Zhu, R. Dong, C. Zhao, G. Li, G. Li, W. Gao, G. Jiang, E. Zheng, G. Cai, S. Moisyadi, J. Urschitz, H. Yang, D. Liu, and Z. Wu. 2017. Production of functional human nerve growth factor from the saliva of transgenic mice by using salivary glands as bioreactors. Sci. Rep. 7:41270.
Zhang, S., J. Shen, D. Li, and Y. Cheng. 2021. Strategies in the delivery of Cas9 ribonucleoprotein for CRISPR/Cas9 genome editing. Theranostics 11:614–648.